Science Advances
AAAS

Supplementary Materials for

Fluoride permeation mechanism of the Fluc channel in liposomes revealed by solid-state NMR

Jin Zhang *et al.*

Corresponding author: Chaowei Shi, scwei@ustc.edu.cn

Sci. Adv. **9**, eadg9709 (2023)
DOI: 10.1126/sciadv.adg9709

The PDF file includes:

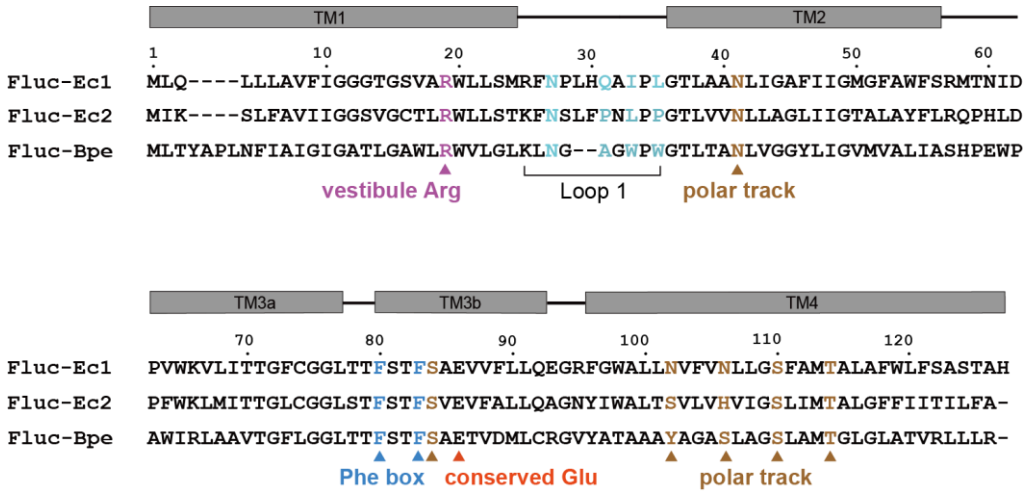

Figure S1. Amino acid sequence alignment of Fluc-Ec1, Fluc-Ec2 and Fluc-Bpe using Fluc-Ec1 amino acid code.

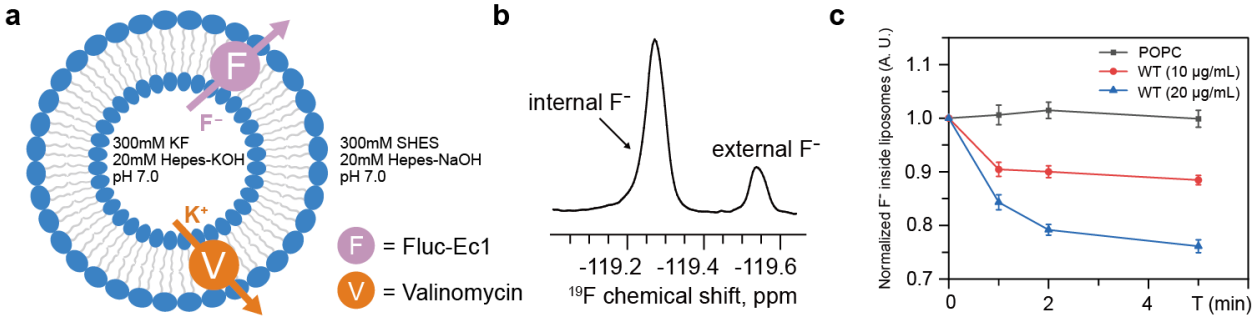

Figure S2. Fluoride efflux from proteoliposomes recorded by ^{19}F-detected solution NMR. All ^{19}F transport assays were performed with POPC loaded with 300 mM KF and suspended in 300 mM SHES (2-Hydroxyethanesulfonic acid sodium salt) at pH 7.0, and fluoride efflux was monitored using ^{19}F solution NMR. (**a**) Schematic showing net KF efflux initiated by valinomycin. (**b**) ^{19}F NMR spectrum of WT Fluc-Ec1 liposomes sample with internal 300 mM KF and external 300 mM SHES spiked with 3 nM F^- at -119.27 ppm and -119.54 ppm respectively.

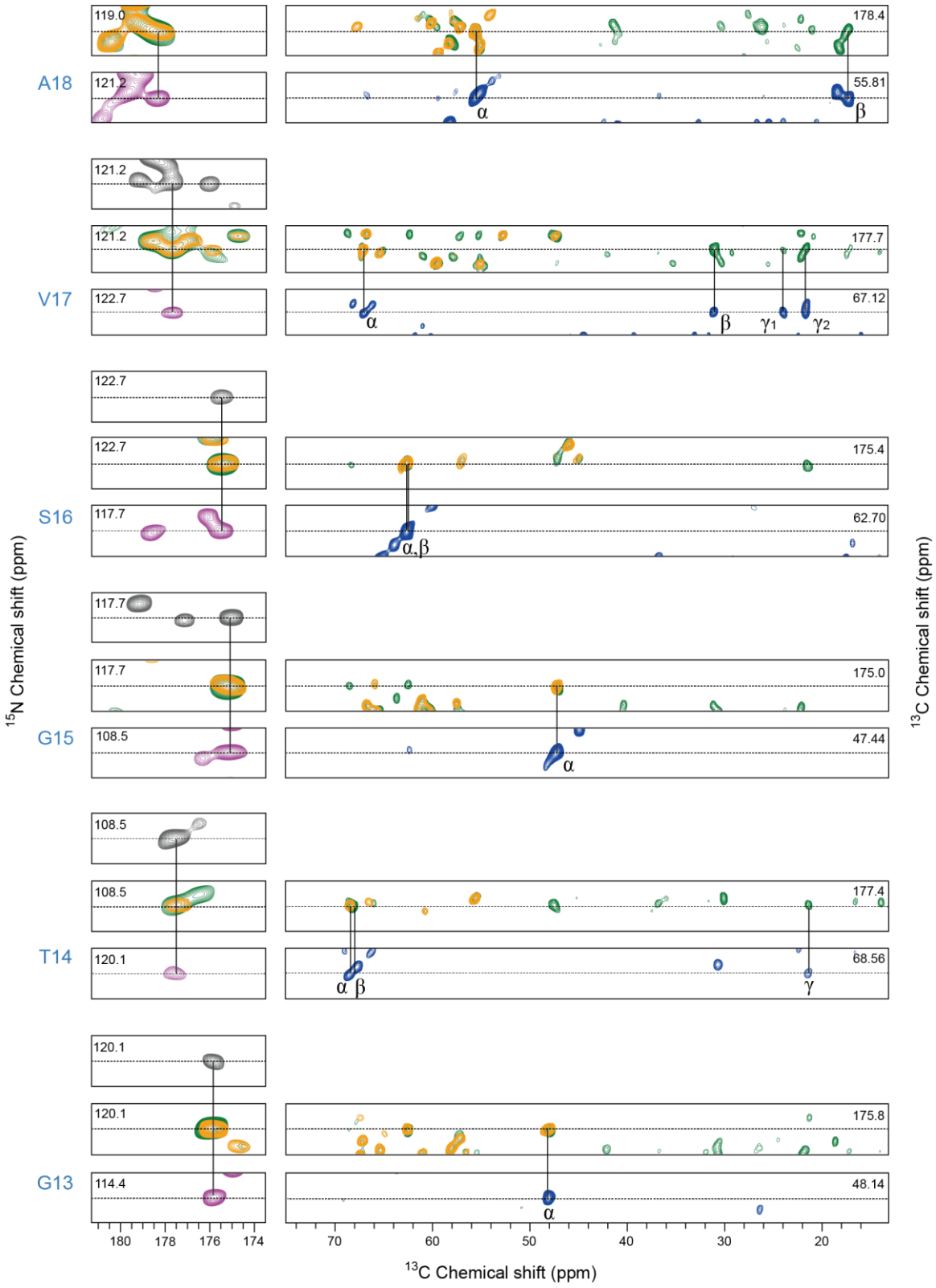

Figure S3. Sequential walk using 3D correlation spectra. Shown are strip plots of 3D NCACX (blue), NCOCX (green), CANCO (grey), NCACO (purple), and NCOCA (orange) spectra analyzed to perform a sequential walk along amino acids Ala18–Gly13. The connections used in the sequential walk are indicated by solid lines. The corresponding nitrogen and carbon chemical shifts are listed.

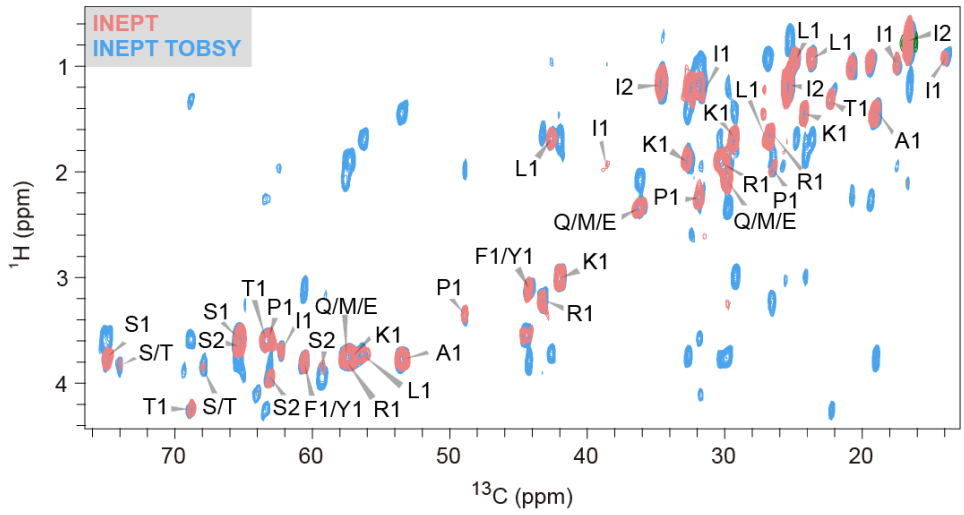

Figure S4. Overlap of scalar based ^{1}H–^{13}C INEPT and INEPT TOBSY spectra of uniformly [^{13}C, ^{15}N]-labeled Fluc-Ec1 in high F^{-} environment. The observed spin systems correlate well to flexible regions from the loop connecting TM2 and TM3a ($_{53}$AWFSRMTNIDPVWKV$_{67}$), N-terminal residue types ($_{1}$MLQLL$_{5}$), and C-terminal residue types ($_{120}$LFSASTAH$_{127}$).

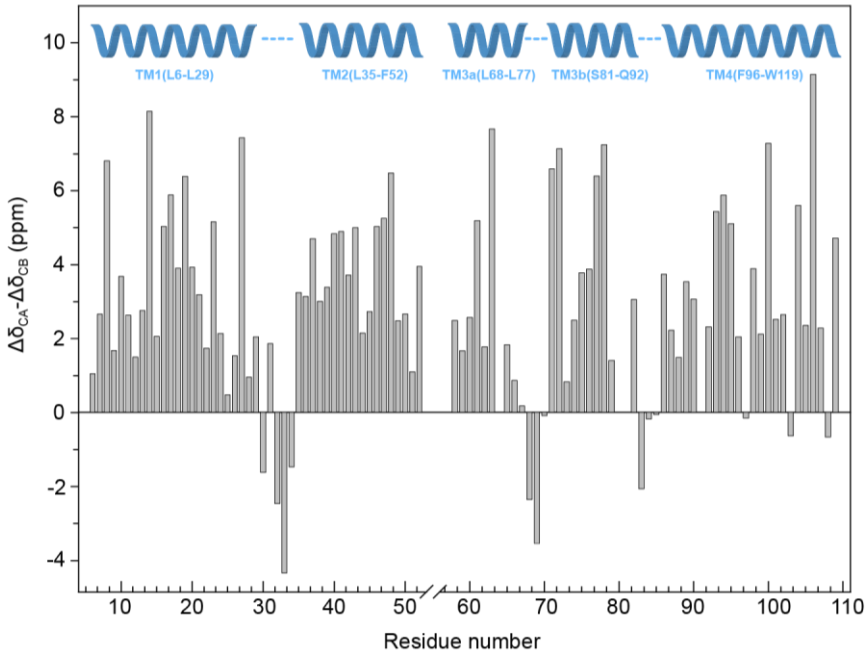

Figure S5. Secondary structure analysis of Fluc-Ec1 by means of secondary chemical shifts. The secondary chemical shifts ($\Delta\delta_{CA}$–$\Delta\delta_{CB}$, in ppm units) are shown as a function of the residue number for the rigid region of Fluc-Ec1, which indicates five continuous α-helices separated by loops (blue dashed line).

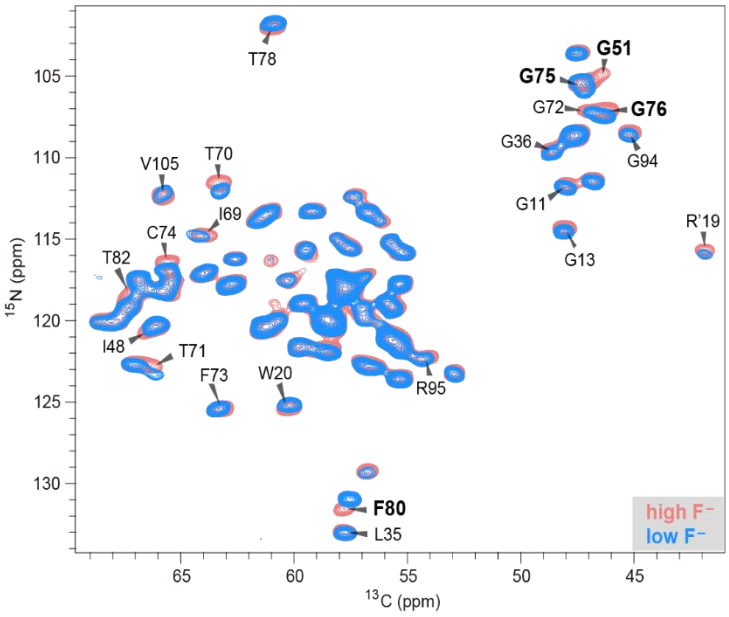

Figure S6. 2D ^{15}N-^{13}CA correlation spectrum comparison of uniformly [^{13}C,^{15}N]-labeled WT Fluc-Ec1 under different fluoride concentration. The spectrum shows assigned peaks with variable chemical shift under high or low F^- concentration, indicated in lightcoral and blue respectively. Residues with notably different chemical shift represent in black and bold fonts as shown in Fig. 2a. The spectrum was recorded on a 16.4 T wide-bore NMR spectrometer at 20 kHz MAS rate.

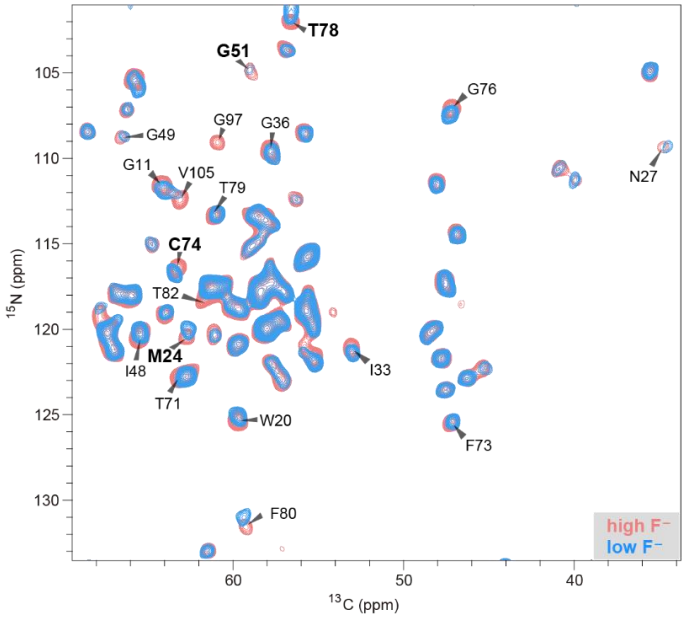

Figure S7. 2D ^{15}N-CO-^{13}CA correlation spectrum comparison of uniformly [^{13}C,^{15}N]-labeled WT Fluc-Ec1 under different fluoride concentration. The spectrum shows assigned peaks with variable chemical shift under high or low F^- concentration, indicated in lightcoral and blue respectively. Residues with notbaly different chemical shift represent in black and bold fonts as shown in Fig. 2b. The spectrum was recorded on a 16.4 T wide-bore NMR spectrometer at 20 kHz MAS rate.

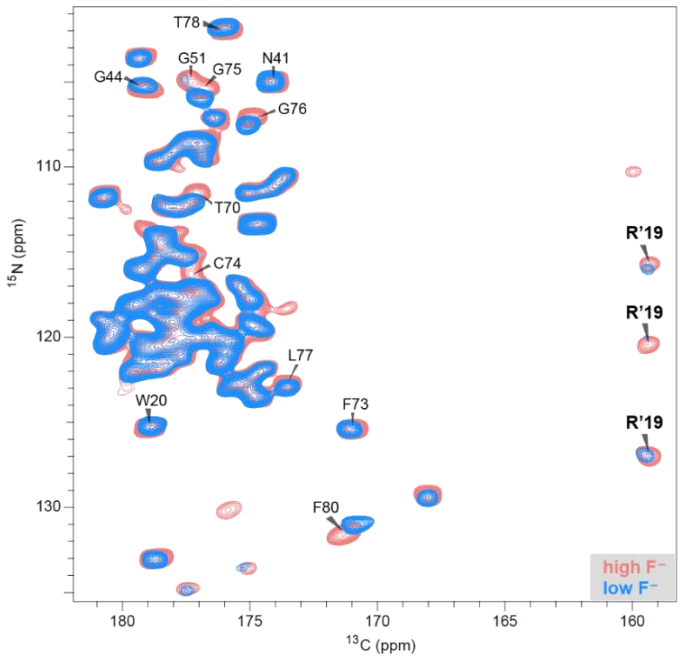

Figure S8. 2D ^{15}N-^{13}CO correlation spectrum comparison of uniformly [^{13}C,^{15}N]-labeled WT Fluc-Ec1 under different fluoride concentration. The spectrum shows assigned peaks with variable chemical shift under high or low F^- concentration, indicated in lightcoral and blue respectively. Residues with notably different chemical shift represent in black and bold fonts as shown in Fig. 2c. The spectrum was recorded on a 16.4 T wide-bore NMR spectrometer at 20 kHz MAS rate.

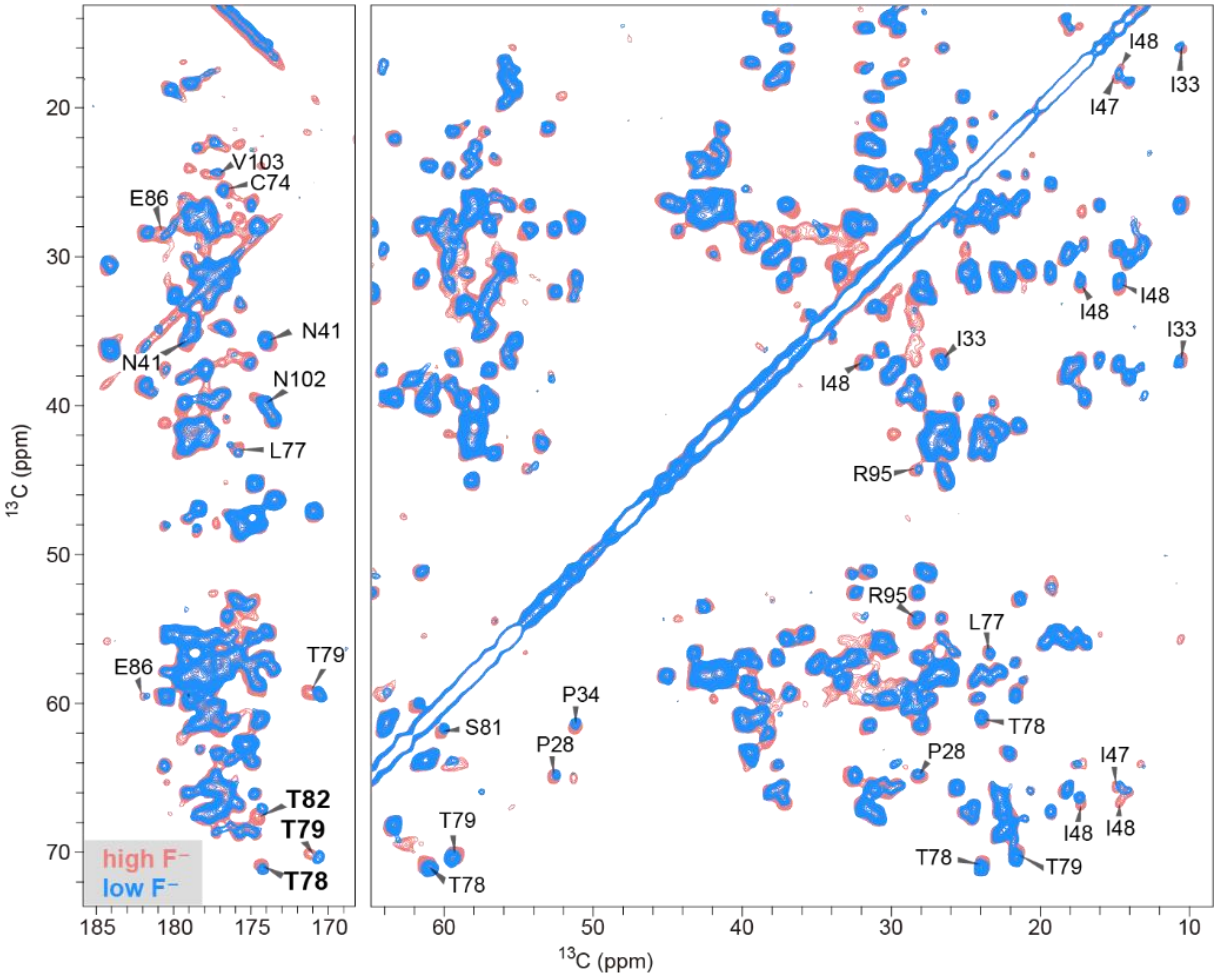

Figure S9. 2D ^{13}C-^{13}C PDSD correlation spectrum comparison of uniformly [^{13}C, ^{15}N]-labeled WT Fluc-Ec1 under different fluoride concentration. The spectrum shows assigned peaks with variable chemical shift under high or low F^- concentration, indicated in lightcoral and blue respectively. Residues with notably different chemical shift represent in black and bold fonts as shown in Fig. 2d. The spectrum was recorded on a 16.4 T wide bore NMR spectrometer at 11 kHz MAS rate. The ^{13}C-^{13}C mixing time was set to 20 ms.

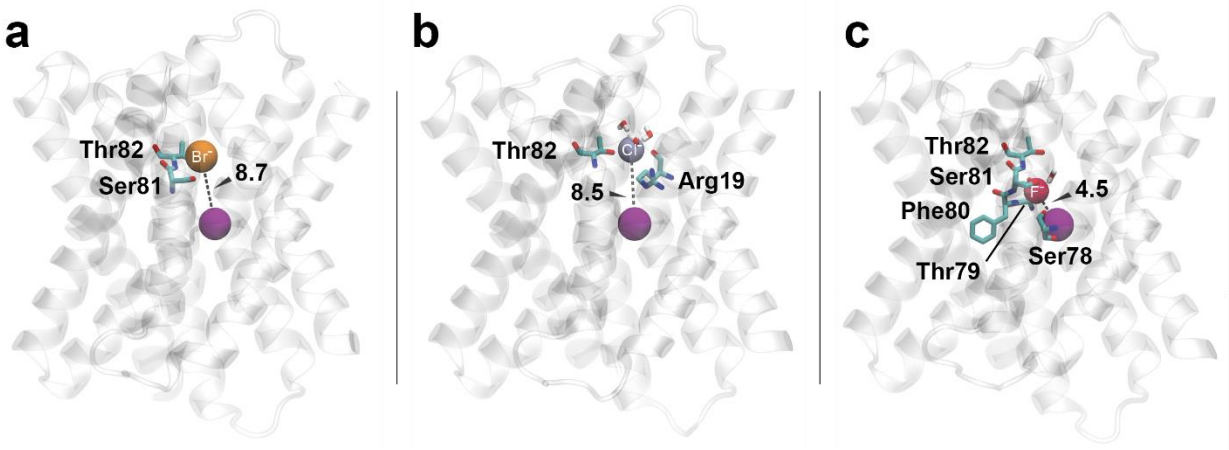

Figure S10. Comparison of the vestibular binding sites of (a) bromide, (b) chloride and (c) fluoride. The structures shown correspond to the Fluc-Ec2 crystal structure with PDB ID 7KKR (**a**) and to a snapshot of the MD simulation with chloride counterions and fluoride bound (**b** and **c**). Distances between bromide, chloride, fluoride and the central sodium (purple sphere) in the vestibule are 8.7 Å, 8.5 Å and 4.5 Å respectively.

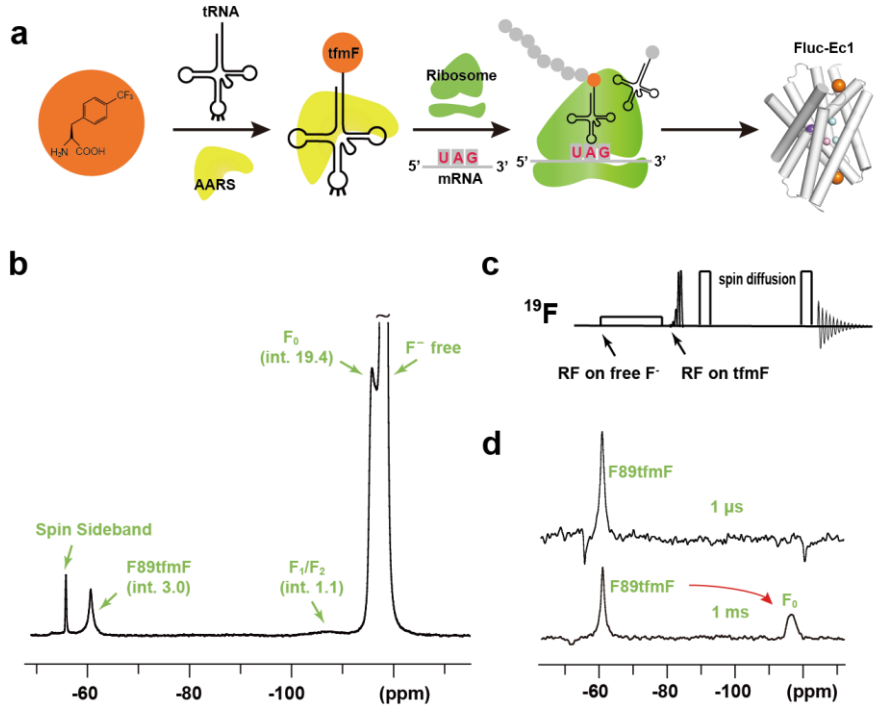

Figure S11. ^{19}F spin diffusion from labeled unnatural amino acid tfmF to fluoride in the vestibule (F_0 sites). (**a**) Schematic diagram showing the mechanism of site-specific incorporation of tfmF into Fluc-Ec1. (**b**) ^{19}F direct excitation spectrum of the tfmF-modified sample in high F^- condition. The integral area sizes are labeled in each bracket, with the CF_3 signal from the F89tfmF used as reference. (**c**) ^{19}F spin diffusion pulse program used for data acquisition. (**d**) Compared ^{19}F spin diffusion spectra with mixing time 1 µs and 1 ms.

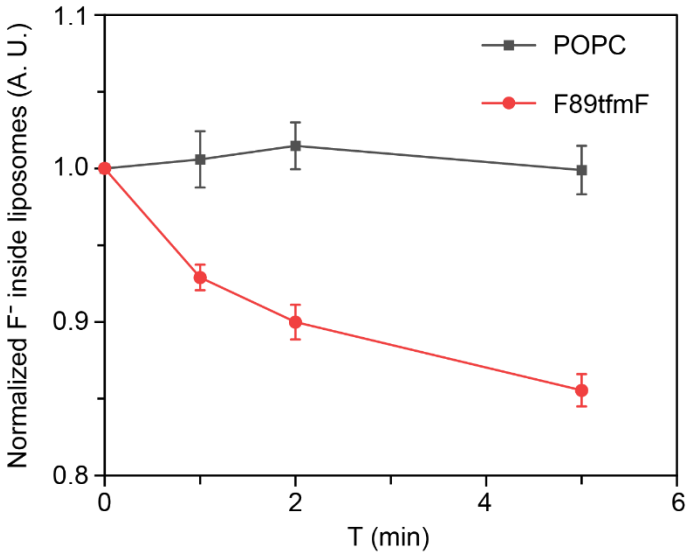

Figure S12. Fluoride transport of Fluc-Ec1 F89tfmF mutant compared to empty POPC liposomes. ^{19}F solution NMR was used to monitor fluoride transport of Fluc-Ec1 F89tfmF mutant. The time-dependent decrease of the internal KF peak showed that reconstituted F89tfmF mutant in liposomes is functional.

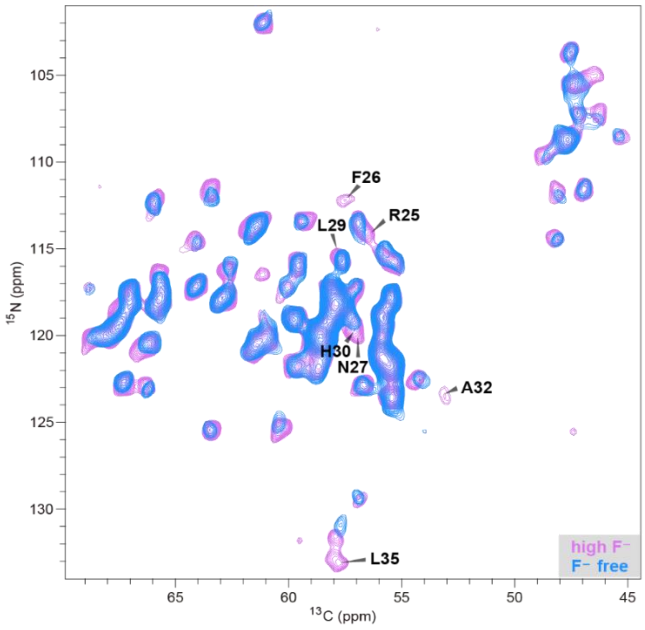

Figure S13. 2D ^{15}N-^{13}CA correlation spectrum overlap of uniformly [^{13}C,^{15}N]-labeled WT Fluc-Ec1 under different fluoride conditions. The spectrum shows assigned peaks with a notable signal intensity decrease in F$^-$-free sample (blue) compared to high-F$^-$ sample (purple). Residues on loop 1 with notable signal intensity decrease represent in black and bold fonts as shown in Fig. 3b. The spectrum was recorded on a 16.4 T wide-bore NMR spectrometer at 20 kHz MAS rate.

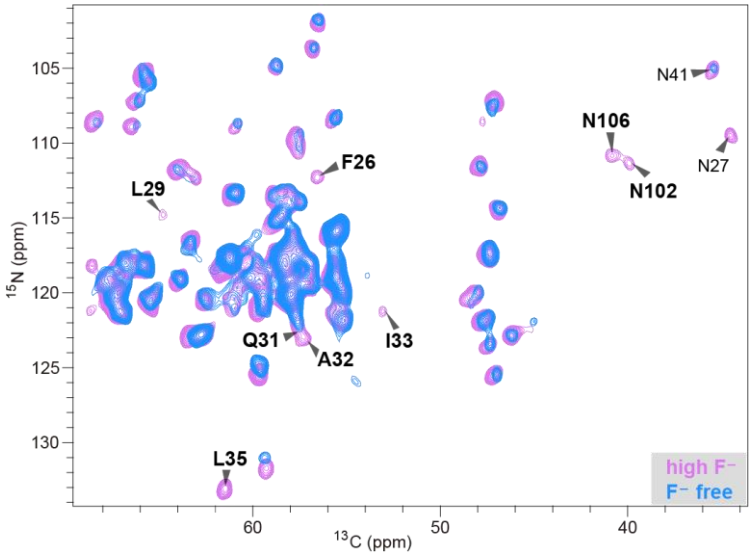

Figure S14. 2D ^{15}N-CO-^{13}CA correlation spectrum overlap of uniformly [^{13}C,^{15}N]-labeled WT Fluc-Ec1 under different fluoride conditions. The spectrum shows assigned peaks with a notable signal intensity decrease in F^--free sample (blue) compared to high-F^- sample (purple). Side chains of Asn102, Asn106 and residues on loop 1 with notable signal intensity decrease represent in black and bold fonts as shown in Fig. 3c. The spectrum was recorded on a 16.4 T wide-bore NMR spectrometer at 20 kHz MAS rate.

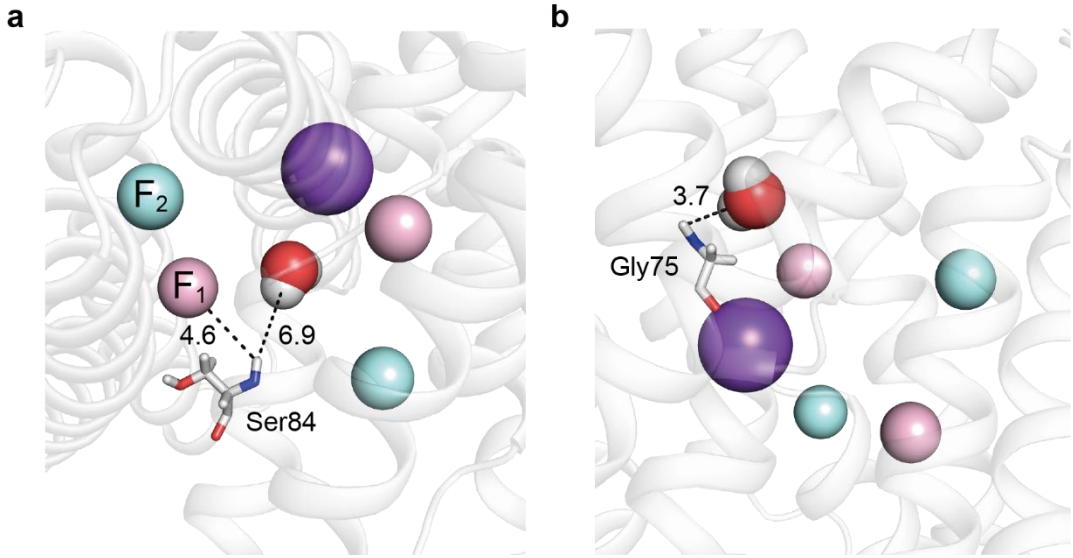

Figure S15. Distances from nearest bound water to Ser84 and Gly75 amide proton. In the Fluc channel crystal structure with the highest resolution (PDB:5NKQ, Bordetella pertussis), residues S86 and G77 (corresponding to S84 and G75 in Fluc-Ec1) amide protons are 6.9 Å and 3.7 Å away from the nearest stably bound water (red spheres) respectively. Molecule at F_1 site (pink spheres, assigned as fluoride in previous crystal structure) exhibits the closer distance 4.6 Å away from Ser84, which is proved to be ^1H_2O instead of fluoride supported by our ssNMR data.

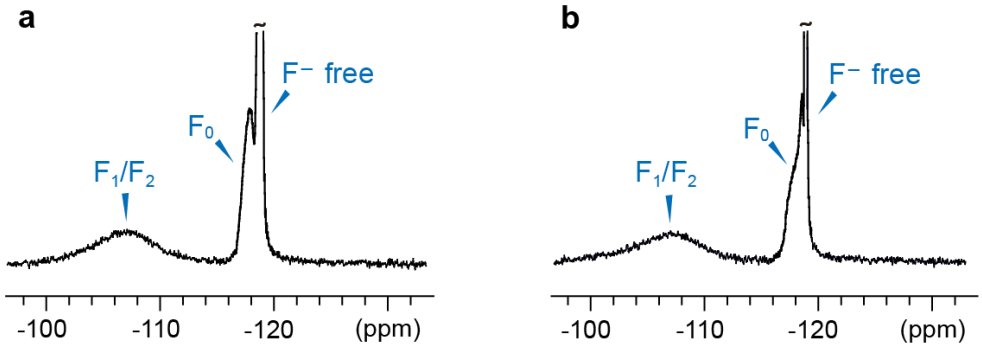

Figure S16. Direct ^{19}F-detected ssNMR spectra of Fluc-Ec1 F80M (a) and F83M (b) mutants under high F$^-$ concentration condition (150 mM NaF).

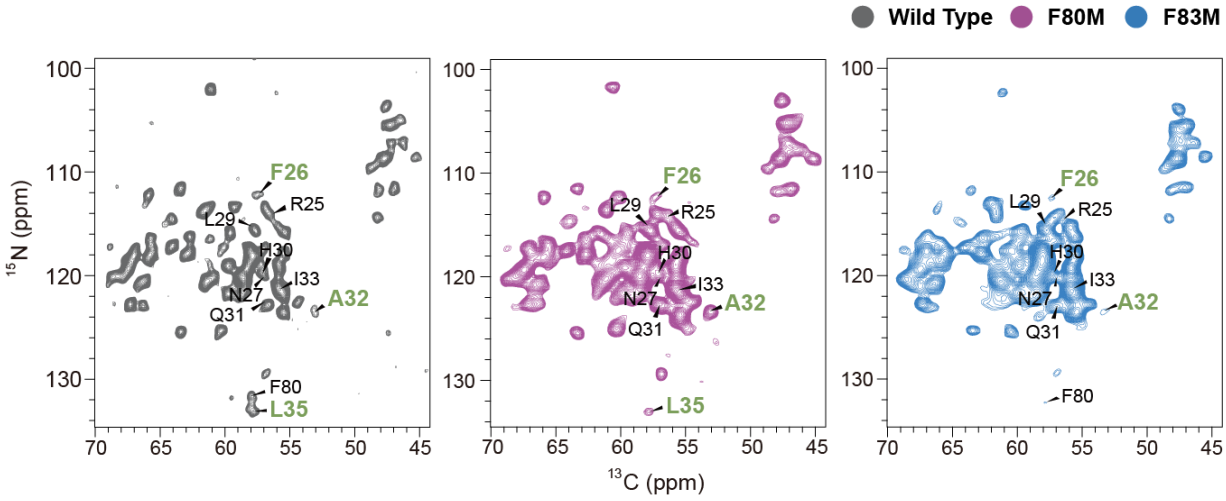

Figure S17. Comparison of 2D ^{15}N-^{13}CA spectra of uniformly [^{13}C,^{15}N]-labeled WT Fluc-Ec1 and variant mutants. The spectra show notable signal intensity decrease at N-CA cross-peaks of F26, A32 and L35 (in green and bold fonts) on loop 1 for F83M (blue contours) compared to WT Fluc-Ec1 (grey contours), while F80M (purple contours) maintains the similar signal intensity as WT Fluc-Ec1.

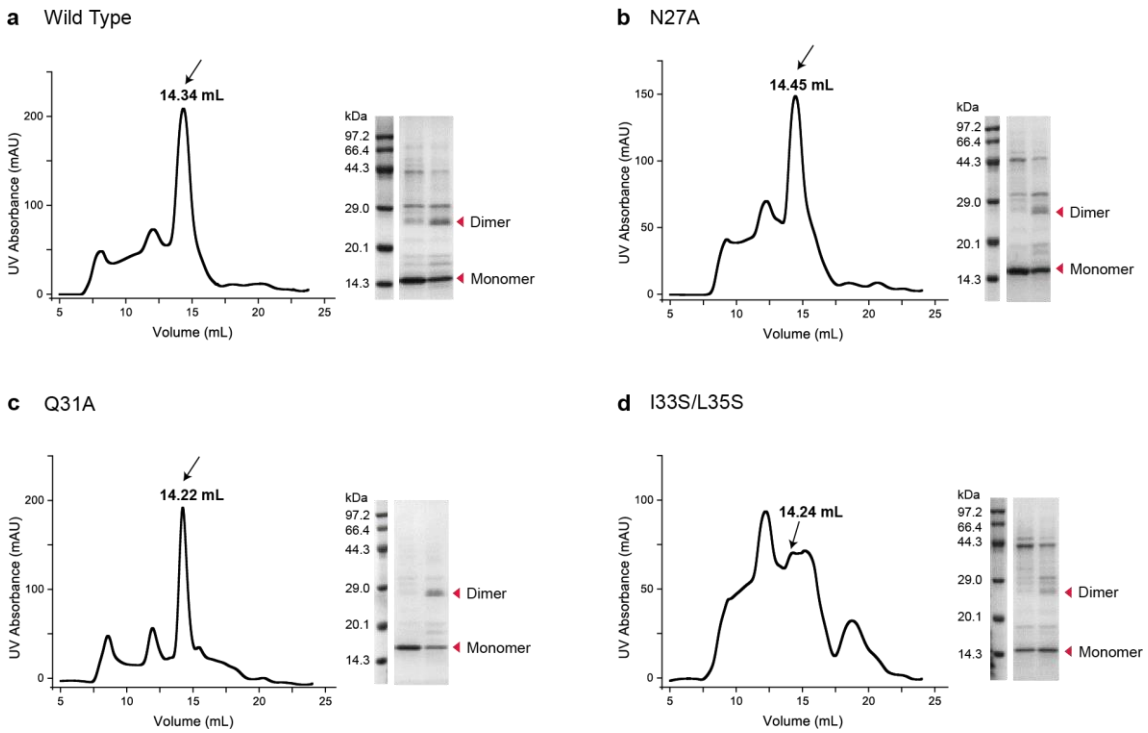

Figure S18. SEC profiles and SDS–PAGE analysis of Fluc-Ec1 WT, N27A, Q31A and I33S/L35S mutants.

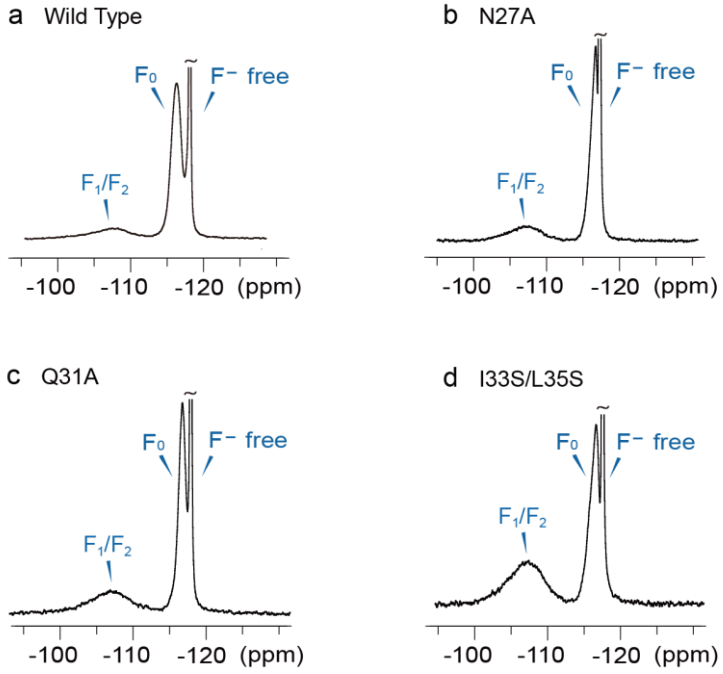

Figure S19. Direct ^{19}F-detected ssNMR spectra of Fluc-Ec1 WT, N27A, Q31A and I33S/L35S mutants under high F^- concentration condition (150 mM NaF).

Table S1. Chemical shift assignments for Fluc-Ec1 in a high F^- concentration environment.

	N	CO	Cα	Cβ	Cγ	Cδ	Other
L6	122.6	174.9	57.28	42.95			
A7	123.4	180.4	55.35	18.61			
V8	119.6	178.4	67.45	30.95	22.72		
F9	120.4	177.9	61.34	41.62			
I10	117.1	180.7	64.13	37.53	29.77/17.65		
G11	111.7	175.0	48.01				
G12	111.4	178.4	46.88				
G13	114.4	175.8	48.14				
T14	120.1	177.4	68.56	67.85	21.90		
G15	108.5	175.0	47.44				
S16	117.7	175.4	62.70	62.77			
V17	122.7	177.7	67.12	31.54	24.51/22.28		
A18	121.2	178.4	55.81	17.82			
R19	119.0	179.0	59.67	27.28	24.18	41.91	Cζ:159.4/NE:79.12 NH1:74.32/NH2:67.72
W20	125.3	177.4	60.29	28.89			
L21	118.0	179.5	57.99	41.52			
L22	118.0	179.2	57.79	42.77			
S23	116.3	175.8	62.62	62.56			
M24	120.2	178.0	58.41	33.18			
R25	114.0	177.8	56.24	29.76	25.37		
F26	112.4	176.8	57.34	37.76			
N27	119.9	177.4	56.95	34.72	176.8		ND2:109.4
P28	134.8	177.6	64.85	32.48	28.24	52.61	
L29	115.0	176.5	58.03	42.70	27.72		
H30	119.3	175.7	57.27	32.65			
Q31	122.6	174.7	57.08	27.87			
A32	123.2	176.1	52.99	21.37			
I33	121.2	175.1	55.57	36.99	26.56/16.05	10.54	
P34	133.5	178.7	61.47	31.53	27.88	51.18	

	N	CO	Cα	Cβ	Cγ	Cδ	Other
L35	133.0	178.4	57.78	41.25			
G36	109.5	175.8	48.52				
T37	120.3	174.7	66.04	68.78	22.75		
L38	118.3	178.2	57.52	41.23			
A39	119.2	178.5	55.68	18.21			
A40	118.8	179.3	55.81	16.89			
N41	115.9	179.2	55.26	35.56	174.0		ND2:105.0
L42	121.7	179.2	58.45	41.45			
I43	118.3	179.2	65.91	37.99	30.18/18.36	14.08	
G44	105.3	174.8	47.53				
A45	123.5	180.5	55.39	18.58			
F46	120.0	177.3	60.79	37.72			
I47	117.4	178.0	65.51	37.33	29.58/18.09	14.89	
I48	120.6	177.0	66.54	37.14	31.8/17.32	14.68	
G49	108.6	174.5	47.86				
M50	121.9	177.4	58.99	33.23			
G51	104.9	173.5	46.48				
F52	118.4	179.3	62.01				
P63			64.97	32.68	27.44	51.29	
L68		178.5	58.47	42.70			
I69	114.8	177.2	64.09	39.50	29.15/17.09	13.26	
T70	111.5	175.6	63.31	68.18	22.09		
T71	122.9	176.4	66.27	68.52	22.32		
G72	107.1	171.0	47.16				
F73	125.4	177.3	63.27	37.56			
C74	116.4	176.7	65.67	25.54			
G75	105.4	174.9	47.22				
G76	107.1	173.6	46.25				
L77	122.8	175.9	56.54	43.08	27.39	25.95/23.51	
T78	102.0	174.5	61.05	70.84	23.86		
T79	113.3	171.3	59.19	70.17	21.60		

	N	CO	Cα	Cβ	Cγ	Cδ	Other
F80	131.6	178.9	57.83	39.87			
S81	113.9	177.0	61.72	60.23			
T82	118.2	174.7	67.34	67.64	21.95		
F83	119.8	174.6	58.89				
S84	113.4	176.4	61.18	63.78			
A85	117.9	177.4	55.42	17.56			
E86	115.7	180.8	59.52	28.39	38.58	181.9	
V87	119.0	177.1	67.29	31.20	25.17/19.31		
V88	120.1	178.0	67.78	30.85			
F89	119.2		59.47				
Q92	120.2	178.0	58.95	28.55			
E93	115.1	176.7	55.78	30.59	36.32	184.2	
G94	108.5	174.8	45.21				
R95	122.3	176.7	54.21	28.26	26.59	44.34	
F96	119.1	178.0	60.88	39.10			
G97	109.1	176.1	47.61				
W98	121.7	179.1	59.7	30.74			
A99	120.9	179.4	55.71	18.09			
L100	118.0		58.01	41.66			
L101		178.2					
N102	117.3	179.6	57.03	39.91	174.1		ND2:111.3
V103	118.1	177.1	66.85	31.72	24.49/22.38		
F104	117.9	178.4	63.07	39.15			
V105	112.4	177.5	65.80	31.00	23.18/20.68		
N106	117.9	176.7	57.77	40.92	173.6		ND2:110.7
L107	117.2	175	58.12	44.99	26.40		
L108	113.3	179.3	56.81	39.64	28.08		
G109	103.6	175.4	47.50				
S110	117.1	175.0	63.94	61.76			
F111	118.8	178.0	57.01	36.45			

	N	CO	Cα	Cβ	Cγ	Cδ	Other
A112	117.6	178.9	55.27	18.54			
M113	115.5	178.7	57.53	35.07	34.00		
T114	117.2	175.8	66.87	68.71	22.44		
A115	121.3	179.5	55.37	18.93			
L116	116.3	178.0	61.01	38.58			
A117	120.2		56.01	19.64			
F118	120.1	178.4	58.42	41.04			
W119	117.6	177.8	60.31	28.12			

Table S2. The distances of each highlighted residues in Figure 4 to F_1, F_2 and the closest crystallographic water. Steric hindrance with monobodies may prevent water approaching Leu35, and the crystallographic water measured in this table to Leu35 may not the closest one in the sample we used.

	F_2	closest crystallographic water	F_1
Leu 35	8.8 Å	6.0 Å	15.4 Å
Cys 74	15.7 Å	5.0 Å	10.1 Å
Gly 75	13.5 Å	3.7 Å	9.6 Å
Gly 76	14.2 Å	5.6 Å	10.5 Å
Thr 78	12.9 Å	5.9 Å	6.9 Å
Thr 79	6.3 Å	6.9 Å	6.0 Å
Phe 83	5.7 Å	5.9 Å	6.7 Å
Ser 84	7.1 Å	6.9 Å	4.6 Å

Table S3. Primers used for molecular cloning.

Primer	Primer sequence (5'→3')
F89tfmF-F	gaagtggtgtagttgttacaagagggtcgctttggctggg
F89tfmF-R	cttgtaacaactacaccacttctgccgaaaatgttgagaagg
F80M-F	caccaccggattttgtggcggtctaacaaccatgtcaacattttcg
F80M-R	gtaacaaaaacaccacttctgccgaaaatgttgacatggttgttagacc
F83M-F	gattttgtggcggtctaacaaccttctcaacaatgtcggcagaagtggtg
F83M-R	ctcttgtaacaaaaacaccacttctgccgacattgttgagaaggttg
N27A-F	aagtatgcgatttgcaccgctgcatcaggcgattccgttgg
N27A-R	atgcagcggtgcaaatcgcatacttaacagccatctcgccacgc
Q31A-F	taacccgctgcatgcagcgattccgttggggacgctg
Q31A-R	caacggaatcgctgcatgcagcgggttaaatcgcatacttaacagcc
I33S/L35S-F	gctgcatcaggcgagtccgtcggggacgctggcagcaaacctgattg
I33S/L35S-R	gccagcgtccccgacggactcgcctgatgcagcgggttaaatcgc